Dalton Transactions

Accepted Manuscript

This article can be cited before page numbers have been issued, to do this please use: T. Stringer, R. Seldon, N. Liu, D. Warner, C. Tam, L. Cheng, K. Land, P. Smith, K. Chibale and G. Smith, *Dalton Trans.*, 2017, DOI: 10.1039/C7DT01952A.

This is an Accepted Manuscript, which has been through the Royal Society of Chemistry peer review process and has been accepted for publication.

Accepted Manuscripts are published online shortly after acceptance, before technical editing, formatting and proof reading. Using this free service, authors can make their results available to the community, in citable form, before we publish the edited article. We will replace this Accepted Manuscript with the edited and formatted Advance Article as soon as it is available.

You can find more information about Accepted Manuscripts in the author guidelines.

Please note that technical editing may introduce minor changes to the text and/or graphics, which may alter content. The journal's standard Terms & Conditions and the ethical guidelines, outlined in our author and reviewer resource centre, still apply. In no event shall the Royal Society of Chemistry be held responsible for any errors or omissions in this Accepted Manuscript or any consequences arising from the use of any information it contains.

ROYAL SOCIETY OF CHEMISTRY

rsc.li/dalton

ROYAL SOCIETY OF CHEMISTRY
View Article Online
DOI: 10.1039/C7DT01952A

Journal Name

ARTICLE

Antimicrobial activity of organometallic isonicotinyl and pyrazinyl ferrocenyl-derived complexes

Received 00th January 20xx,
Accepted 00th January 20xx

DOI: 10.1039/x0xx00000x

www.rsc.org/

Tameryn Stringer[a], Ronnett Seldon[b], Nicole Liu[c], Digby F. Warner[d,e], Christina Tam[f], Luisa W. Cheng[f], Kirkwood M. Land[c], Peter J. Smith[g], Kelly Chibale[a,b] and Gregory S. Smith[a,*]

Isonicotinyl and pyrazinyl ferrocenyl-derived complexes were prepared using various hydrazides and ferrocenyl aldehydes. Three heterobimetallic complexes were also synthesized from the Schiff base-derived isonicotinyl ferrocene complex using various platinum group metal dimers based on ruthenium, rhodium and iridium. All complexes were evaluated *in vitro* for antimycobacterial and antiparasitic activity. Against *Mycobacterium tuberculosis* H37Rv, the platinum group metal complexes showed glycerol-dependent antimycobacterial activity. The antiplasmodial activities against the NF54 chloroquine-sensitive strain of *Plasmodium falciparum* of some compounds were moderate, while some complexes also showed promising activity against *Trichomonas vaginalis*. Incorporation of the ferrocenyl-salicylaldimine moiety resulted in enhanced antimicrobial activity compared to the non-ferrocenyl compound in some cases. The bimetallic iridium-ferrocene isonicotinyl complex exhibited superior antitrichomonal activity relative to its organic counterpart, isoniazid. Furthermore, all these compounds, when screened on several normal flora bacteria of humans, showed no effect on the microbiome, emphasizing the selection of these compounds for these pathogens. The promising antimicrobial activities of the complexes thus supports incorporation of ferrocene as part of existing antimicrobial therapies in order to alter their biological activities favorably.

Introduction

The development of organometallic compounds as potential medicinal agents has been on the rise for the past decade.[1-3] Although the field of bioorganometallic anticancer studies remains one of the most prevalent research areas, recent advances in other fields have also generated scientific interest.[4] Ferrocene and ferrocene-derived molecules have interesting biological properties. For example, the replacement of an aromatic group in penicillin by ferrocene resulted in a compound comparable in activity to benzyl penicillin.[5,6] Ferrocene-containing compounds also exhibit antiproliferative activities.[7-10] Hydroxyferrocifen shows promising antiproliferative activity against various breast cancer cell lines. In addition to this, ferrociphenols and hydroxypropyl ferrociphenols show antiproliferative effects against triple negative breast cancer cells.[11-14] The ferrocenyl fragment often brings about a metal-specific mechanism of action. Since Fe(II) is redox active, the ferrocenyl moiety is able to generate reactive oxygen species (ROS). In addition to this, incorporation of ferrocene can alter the permeability of the compound by altering the lipophilicity. Very recently, the antiparasitic activity of metallocene and ferrocenyl-monepantel derivatives were reported against *Trichostrongylus colubriformis* and *Dirofilaria immitis* microfilariae.[15,16] The versatility of the ferrocenyl moiety in biological applications and the incorporation of ferrocene

[a]*Department of Chemistry, University of Cape Town, Rondebosch, 7701, Cape Town, South Africa*
[b] *Drug Discovery and Development Centre (H3-D), Department of Chemistry, University of Cape Town, Rondebosch, 7701, South Africa*
[c] *Department of Biological Sciences, University of the Pacific, Stockton, CA 95211, USA*
[d] *MRC/NHLS/UCT Molecular Mycobacteriology Research Unit, DST/NRF Centre of Excellence for Biomedical TB Re-search, Department of Pathology, University of Cape Town, Rondebosch, 7701, Cape Town, South Africa*
[e] *Institute of Infectious Disease and Molecular Medicine, University of Cape Town, Rondebosch, 7701, Cape Town, South Africa*
[f]*Foodborne Toxins Detection and Prevention Research Unit, Agricultural Research Service, United States Department of Agriculture, Albany, CA, 94710, USA*
[g]*Division of Pharmacology, Department of Medicine, University of Cape Town, Medical School, Observatory, 7925, Cape Town, South Africa*
**G.S.S.: e-mail, gregory.smith@uct.ac.za; web, www.gregsmith-research.co.za; tel, +27 21 650 5279.*
Electronic Supplementary Information (ESI) available: [NMR and LC data].

into organic molecules can introduce specific properties such as ROS production, redox activation and lipophilicity. This supports the incorporation of ferrocene for the development of new and more effective clinical agents as a viable approach, especially in the lesser-researched field of antimicrobial agents.

Tuberculosis (TB) is an infectious disease that has been under-explored in terms of potential metal-based therapies. The World Health Organization (WHO) reported an estimated 10.4 million new cases and 1.4 million deaths in 2015 worldwide.[17] Moreover, the increasing incidence of drug resistance has raised concerns about the treatment of this disease. In 2015, 480 000 cases of multidrug resistant (MDR)-TB were reported, which is defined as resistance to rifampicin and isoniazid.[18] In order to circumvent drug resistance, suitable therapeutic alternatives are required for treatment of this disease. In this regard, ferrocenyl diamines (Figure 1a) were evaluated for antimycobacterial activity against the fully drug-susceptible laboratory strain, *M. tuberculosis* H37Rv, and showed potent activities *in vitro*.[19] Based on this, ferrocenyl-containing polyamines (Figure 1b) were prepared and evaluated for antimycobacterial activity.[20] Examples of ferrocene-conjugates of front-line antimycobacterials have not been studied extensively.

Trichomoniasis is a parasitic disease that is caused by the parasite *Trichomonas vaginalis*. The current treatment, metronidazole, has shown decreased efficacy against some clinical isolates in patients.[21,22] As a consequence, there has been an interest in obtaining suitable alternative therapies for this infection.[22] Due to the robust nature of ferrocene, its low toxicity and redox properties,[23,24] we have previously reported on the antitrichomonal activity of ferrocenyl complexes (Figure 1c) that exhibit promising in vitro activity against this protozoan.[25-28]

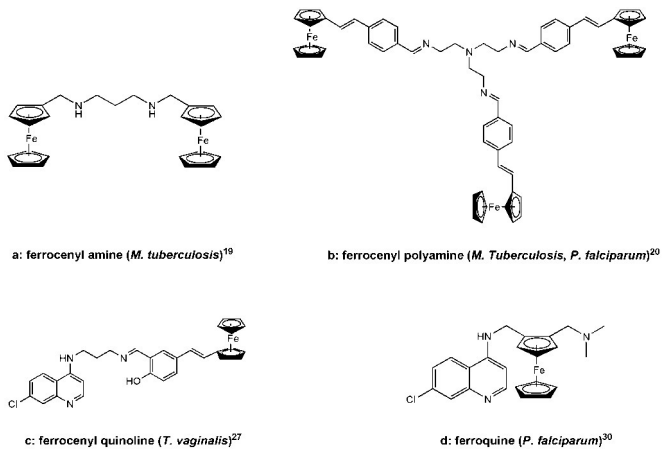

Fig. 1 Ferrocenyl complexes with demonstrated antimicrobial activity.

Malaria is an infectious disease that in 2013 affected over 198 million people worldwide.[29] The species of parasite responsible for the most severe malaria infections is *Plasmodium falciparum*. As a consequence of increased resistance of the parasite towards current drug treatments, alternative therapies are required. Within the context of malaria, the most promising ferrocene-based agent to date is ferroquine (FQ, Figure 1d), which is active against chloroquine (CQ) resistant strains of the causative parasite species and is now in Phase IIb clinical trials, having been reinitiated in 2015 in a new combination with artefenomel.[31,32] Based on this, many quinoline-based ferrocenyl complexes have been evaluated extensively for antiplasmodial activity and have shown promising activity.[32-34] Again, this supports the development of ferrocene-based complexes as potential antimicrobial agents. To the best of our knowledge, ferrocene-based isoniazid/pyrazinyl complexes have not been investigated as potential antiplasmodial or antitrichomonal agents. Herein, we report the synthesis, characterization and antimicrobial activity of a small family of ferrocene-derived isoniazid and pyrazinamide complexes and three isonicotinyl half-sandwich heterobimetallic complexes.

View Article Online
DOI: 10.1039/C7DT01853A

Results and discussion

Synthesis and characterization

The preparation of the ferrocenyl complexes **1** – **6** firstly required the synthesis of the antimycobacterial precursor compounds. Pyrazinoic acid hydrazide (Scheme 1) was prepared from pyrazinoic acid using published methods.[35,36] Methyl pyrazinoate was prepared via an acid-catalyzed esterification, using MeOH. The ester was then treated with hydrazine hydrate to afford the desired hydrazide. Ferrocenyl-containing aldehydes were used in the synthesis of **1** – **6** in order to investigate the effect of the aryl moiety on biological activity. Ferrocenyl aldehydes (**B** and **C**, Scheme 1) were prepared according to literature procedures.[20,27] The preparation involves a Heck cross-coupling reaction of vinylferrocene with either 4-iodobenzaldehyde or 5-iodosalicylaldehyde giving rise to aldehydes **B** and **C**, respectively. Pyrazinoic acid hydrazide and isoniazid were then reacted with ferrocenecarboxaldehyde (**A**) and the aryl ferrocenyl-aldehydes (**B** and **C**) via a Schiff base condensation reaction (Scheme 2) to yield the ferrocenyl complexes (**1** – **6**) as red/orange solids in low to moderate yields (32-56%). Complex **1** was prepared as described in the literature.[37] The complexes were characterized by ^{1}H and $^{13}C\{^{1}H\}$ Nuclear Magnetic Resonance (NMR) and infrared (IR) spectroscopy, electron impact (EI) or electrospray ionization (ESI) mass spectrometry and elemental analysis.

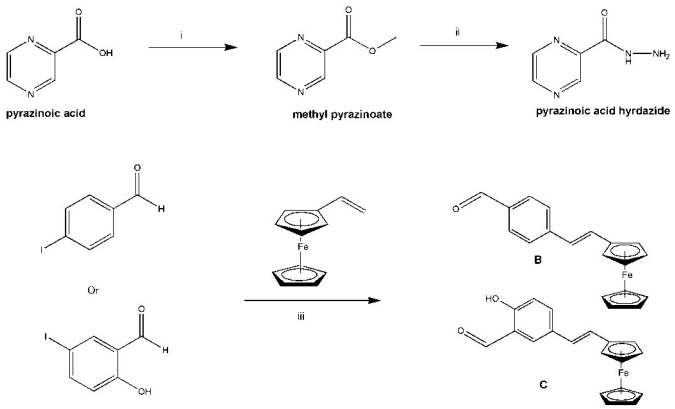

Scheme 1 Preparation of precursors: i) MeOH, H_2SO_4; ii) $NH_2NH_2.xH_2O$; iii) tri(*p*-tolyl)phosphine, $Pd(OAc)_2$, Et_3N, CH_3CN, 24 h, 90 °C.

View Article Online
DOI: 10.1039/C7DT01953A

Successful Schiff base condensation of **2**-**6** was confirmed by a singlet for the imine proton in the region between 8.46 and 8.71 ppm in the ^{1}H NMR spectra. Signals for the ferrocenyl Cp protons were observed in the expected region between 4.14 and 4.77 ppm. The ^{1}H NMR spectra of complexes **2**, **3**, **5** and **6** showed two doublets for each proton of the olefinic moiety, has coupling constants ranging between 14 and 16 Hz which suggested a trans geometry about the double bond, consistent with data obtained for similar structures.[20,27,38] The infrared spectra of the ferrocenyl complexes showed absorption bands between 1605 and 1633 cm^{-1} for the C=N stretching frequencies. Absorption bands for the carbonyl stretching frequencies were observed between 1660 and 1690 cm^{-1}, confirming the amido-form of complexes **2**-**6** in the solid state. A molecular ion peak was observed for each complex in the EI mass spectra confirming the structural integrity of complexes **2** – **6**.

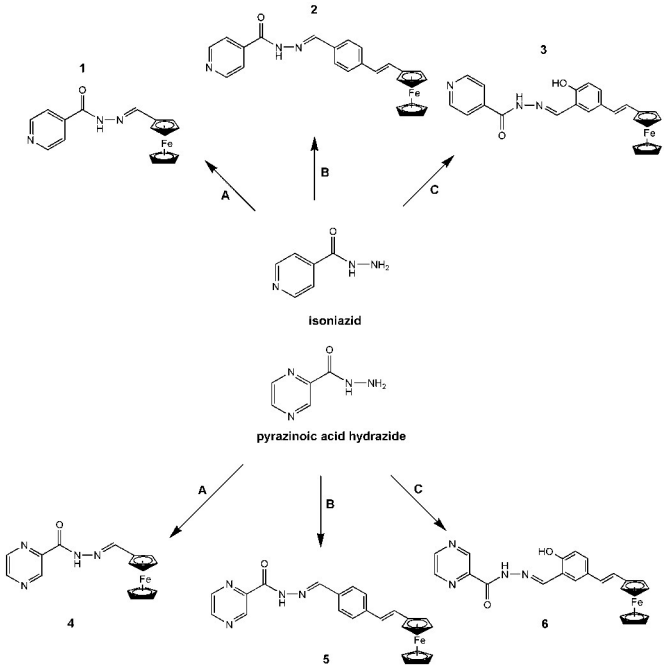

Scheme 2 Preparation of ferrocenyl complexes **1** – **6**: Ferrocenyl aldehyde (**A**, **B** or **C**: 1 eq.), EtOH, reflux, 16 hours.

Half-sandwich complexes, specifically ruthenium compounds have generated interest owing to their lower toxicity compared to platinum-based drugs and their suitability as alternatives for chemotherapy.[1] The half-sandwich complexes (**7**-**9**) were prepared by reacting ferrocenyl complex **1** with either $[IrCp^*Cl_2]_2$, $[RhCp^*Cl_2]_2$ or $[Ru(p\text{-cymene})Cl_2]_2$, in the presence of NaH (Scheme 3) to yield the complexes as orange solids in high yields (>80%). The ^{1}H NMR spectra of **7**–**9** suggests bidentate coordination of the ligand due to the disappearance of the amido proton, which confirms its deprotonation in the presence of the base and coordination via the deprotonated imidic form of the ligand. In the case of complex **9**, further evidence of bidentate coordination as attested to by the chiral nature of the ruthenium metal. Two doublets were observed for the protons of the isopropyl moiety. The protons of the arene moiety also appeared distinct, a consequence of the chiral metal centre. These observations were consistent with similar chiral ruthenium arene complexes.[39-45] Since the mode of coordination was similar for the rhodium and iridium complexes, these complexes were also designated as chiral. Further evidence of this mode of coordination was seen in the infrared spectra. A strong absorption band was observed at approximately 1590 cm^{-1} in each case. The disappearance of the C=O absorption band, suggested a change in the tautomeric form of the ligand from the amide to the imidic form upon complexation, further supporting the proposed structures. The ESI mass spectrum of **9** confirmed that **9** was prepared, as a base peak for the protonated molecular ion was observed. EI mass spectrometry also confirms the integrity of the proposed structures, owing to the observation of the molecular ion peak, in the mass spectra of **7** and **8**.

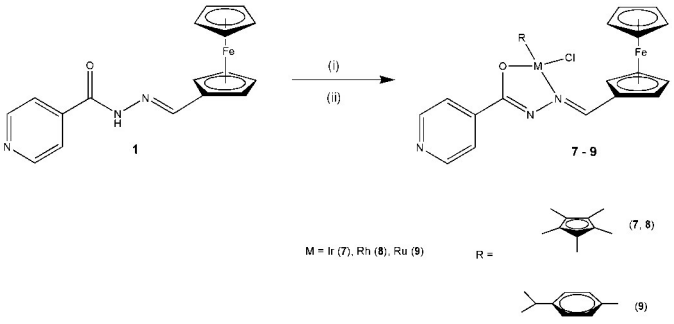

Scheme 3 Preparation of PGM complexes **7** – **9**: (i) DCM, NaH, 1.5 hours, (ii) DCM, $[MCl_2R]_2$, 1.5 hours.

Antimycobacterial activity and cytotoxicity

The synthesized complexes (**1** – **9**) were screened for activity against *M. tuberculosis* H37Rv *in vitro*. Ferrocenyl complexes of isoniazid and the pyrazinoic acid hydrazide precursor were screened in order to evaluate the effect of ferrocene on antimycobacterial activity. In addition to this, half-sandwich (Ir, Rh and Ru) complexes of the ferrocenyl-isoniazid conjugate (**1**) were prepared to determine the effect on antimycobacterial activity by incorporating a second metal. The data are presented in Table 1.

All of the compounds were screened against *M. tuberculosis* H37Rv::gfp in two different growth media – the glycerol-based GAST-Fe (which does not contain bovine serum albumin) and a glucose-based Middlebrook 7H9-ADC (which does contain BSA supplement) - to elucidate any condition-selective antimycobacterial activity. The majority of the compounds tested exhibited potent activity in GAST-Fe medium, giving minimum inhibitory concentration (MIC_{90} and MIC_{99}) values lower than 1 µM on day 14. Isoniazid exhibited similar activity profiles in both media. Complex **2** exhibited lowered activity compared to complex **1** in both media. Isoniazid complexes **2** and **3** showed reduced activity in both growth media compared to isoniazid itself and complex **1**, perhaps as a consequence of higher lipophilicity (Table 2). In most cases, especially for PGM complexes (**7** – **9**), there appeared to be a glycerol-dependent inhibitory activity as the MICs increased when the glucose-based 7H9 medium was used. This was

View Article Online
DOI: 10.1039/C7DT01053A

also observed for complex **1**. This profile was analogous to the glycerol-dependent control, and suggested that the PGM complexes and complex **1**, may exert their inhibitory effects by disrupting glycerol metabolism, resulting in toxic accumulation of intermediate metabolites.[46-50] Selected complexes (**1**, **2** and **8**) were tested against the *M. tuberculosis* cytochrome *bd* oxidase deletion mutant, Δ*cyd*KO (Table 1), to establish whether cytochrome *bc*1 oxidase was a potential cellular target. No hypersensitivity was observed towards Δ*cyd*KO. In addition to this, a Δ*cyd*KO deletion mutant carrying an Ala317Thr point mutation in *qcrB*[51] was also screened using the GAST/Fe assay. No significant differences in the MIC values were observed between the two mutants (unlike the control *qcrB* inhibitor), suggesting that these compounds may not target the *qcrB* subunit of the respiratory *bc*1 complex in *M. tuberculosis*. Compounds that exhibit significant differences between the MIC values of Δ*cyd*KO and *qcrBA*317T, are believed to target this pathway.[52]

Selected compounds were also screened in vitro for mammalian cytotoxicity against Chinese Hamster Ovarian (CHO) cells, using emetine as the control. All of the complexes exhibited lower toxicity than the control (IC_{50} = 0.057 μM) at the tested concentration. This indicated selectivity of the compounds toward *M. tuberculosis*, with two of the isoniazid-ferrocenyl complexes (**2** and **3**) exhibiting only mild toxicity (IC_{50} > 20 μM). However, as noted above, further insight is required into the mechanism of action of these complexes which appear to exhibit growth medium-dependent inhibition.

Table 1 Activity of complexes **1**-**9** against *M. tuberculosis* H37Rv and cytotoxicity against CHO cells

Complex	MIC_{90} (μM) [Media: Gaste Fe]	MIC_{99} (μM) [Media: Gaste Fe]	MIC_{90} (μM) [Media: 7H9 GLU ADC]	MIC_{99} (μM) [Media: 7H9 GLU ADC]	Alamar Blue Assay: MIC_{99} (μM): *Δcyd*KO Gaste Fe	Alamar Blue Assay: MIC_{99} (μM): qcrBA317T Gaste Fe	MTT Assay Cytotoxicity CHO cells: IC_{50} (μM)
1	0.39	0.474	7.29	> 10	0.976	0.976	n.a.[c]
2	> 10	> 10	> 10	> 10	3.906	1.953	> 20
3	41.3	> 125	> 125	> 125	n.d.[b]	n.d.	> 20
4	45.6	120	> 125	> 125	n.d.	n.d.	n.a.
5	> 125	> 125	> 125	> 125	n.d.	n.d.	n.a.
6	> 125	> 125	> 125	> 125	n.d.	n.d.	n.d.
7	0.416	0.6	> 125	> 125	n.d.	n.d.	n.d.
8	0.968	1.47	> 10	> 10	0.976	3.906	n.a.
9	0.514	0.751	> 125	> 125	n.d.	n.d.	n.d.
isoniazid	< 0.244	< 0.244	0.856	1.26	n.d.	n.d.	n.a.
rifampicin	0.00811	0.0295	0.00459	0.0227	0.009	0.009	n.d.
GDC[a]	n.d.	1.19	n.d.	> 125	n.d.	n.d.	n.d.
emetine	n.d.	n.d.	n.d.	n.d.	n.d.	n.d.	0.057 ± 0.004
***qcrb* inhibitor**	n.d.	n.d.	n.d.	n.d.	< 0.204	15.625	n.d.

[a]Glycerol-dependent control
[b]not determined
[c]not active at the highest concentration tested (100 ug mL^{-1})

Table 2 Predicted logP values for **1** – **6** and isoniazid

Compound	ClogP[a]
1	1.75
2	4.59
3	4.22
4	0.73
5	3.57
6	3.21
7	n.d.[b]
8	n.d.
9	n.d.
Isoniazid	-0.69

[a] logP values predicted using MarvinSketch V5.9.4 according to the method described in reference 25 (values do not take into account possible intramolecular H-bonding)
[b]not determined

Antitrichomonal activity

Metronidazole has been the preferred drug used to treat trichomoniasis, since its introduction in 1960.[53] Although resistance to metronidazole has been reported, the drug is still effective, successfully treating more than 90% of infections. However, it does not cure all patients, and resistance is on the rise.[54] The antitrichomonal activities of complexes (**1** – **9**) were evaluated against the G3 isolate of *T. vaginalis* at a 50 µM drug concentration. The results are presented in Figure 2. Given that *T. vaginalis* is a mucosal pathogen that exists within a complex microbiome, screening of all of these compounds on several common normal flora bacteria found within the human microbiome at the highest concentration did not show any effect.

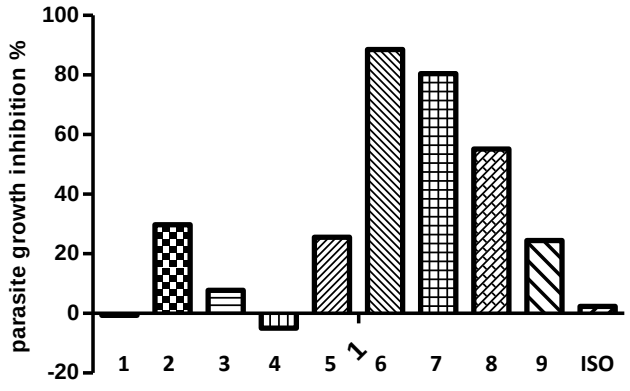

Figure 2 Antitrichomonal activity of complexes (**1** – **9**) and isoniazid against *T. vaginalis*.

All of the tested compounds, with the exception of **6** and **7**, displayed moderate to low parasite growth inhibition. The ferrocenyl-pyrazinamide complex **6** possessed the highest growth inhibitory activity of all of the tested compounds resulting in 88.2% inhibition. Complex **7**, the iridium Cp* complex, exhibited less potent parasite growth inhibition at 80.4%, but this was higher than the rhodium and ruthenium counterparts. Compounds **6** and **7** exhibited promising inhibition, but were not comparable to metronidazole at the same test concentration (data not shown - 100% inhibition). In addition, the water-soluble isoniazid demonstrated very low inhibition along with complexes **1** and **4**. The two benzylaldimine-ferrocenyl complexes (**2** and **5**) exhibited moderate activity, while the pyrazinamide salicylaldimine-ferrocenyl complex **6** possessed much greater activity than its isonicotinyl derivative (**3**). This further supported the use of more lipophilic complexes as antitrichomonal agents, an observation consistent with data obtained in previous studies.[25-28] The IC_{50} values of complex **6** and **7** were elucidated and are given in Table 3. The complexes were far less active than metronidazole at the tested concentration, but could be modified structurally in future to afford suitable leads.

Table 3 IC_{50} values of compounds **6**, **7** and metronidazole against the G3 strain of *T. vaginalis.*

Compound	IC_{50} (µM)[a]
6	10.41
7	14.27
metronidazole	0.72

[a] IC_{50} represents the micromolar equivalents required to inhibit parasite growth by 50%.

Antiplasmodial activity and β-Haematin inhibition

The antiplasmodial activity of compounds **1** – **9** along with isoniazid were evaluated in vitro against the chloroquine-sensitive (CQS) *P. falciparum* NF54 strain using the pLDH (*Plasmodium* lactate dehydrogenase) assay. CQ was used as the reference drug in each case and the data obtained from this study is summarized in Table 4.

Table 4 Antiplasmodial activity of compounds **1** – **9,** isoniazid and CQ against the NF54 CQS strain of *P. falciparum*.

Compound	IC_{50} ± SE (µM)
1	> 100
2	31.52 ± 6.41
3	1.58 ± 0.01
4	> 100
5	10.36 ± 2.81
6	3.77 ± 0.86
7	5.00 ± 0.39
8	2.99 ± 0.75
9	7.82 ± 0.99
Isoniazid	n.a.

chloroquine	0.0149 ± 0.001

[a] not active at the tested concentration

All of the tested compounds exhibited lower activity compared to CQ, in most cases being more than 100-fold less active. Comparing the free ferrocenyl ligands (**1** – **6**), the isoniazid complex **3** exhibited the highest activity in the series as well as overall. Both complexes derived from ferrocenecarboxaldehyde (**1** and **4**) showed low activity with IC_{50} values greater than 100 µM. This is possibly a consequence of the lower lipophilicity of these complexes compared to the rest of the compounds. For the isonicotinyl and pyrazinyl moieties, the isonicotinyl ligand **3** appeared to display enhanced activity compared to the pyrazinyl ligand **6**. Also, the addition of the salicylaldimine-ferrocenyl moiety seemed to be beneficial for antiplasmodial activity. This was evident in the lower activity of **2** and **5** compared with **3** and **6**, respectively. For the heterobimetallic complexes (**7** – **9**), the Rh-Cp* complex (**8**) displayed enhanced activity compared to the ruthenium (**9**) and iridium (**7**) derivatives. Most of the complexes exhibited higher activity compared to isoniazid at the tested concentration, which suggested a positive influence on antiplasmodial activity when ferrocene as well as a second metal was incorporated. There did not appear to be any significant trend with respect to antiplasmodial activity in general for complexes **1** – **6**. The weak cytotoxicity in CHO cells indicated that the activity of the complexes may not be due to general toxicity but rather to a specific *Plasmodium falciparum*-based mechanism, which was further investigated.

The ability of selected compounds (**3**, **4**, **8** and isoniazid) to inhibit β-haematin formation was examined using a detergent-mediated assay[55] to gauge some idea of a possible mechanism of action, despite possessing relatively low antiplasmodial activity. Many quinoline-based compounds are believed to target haemozoin formation in the parasite and therefore it would be worthwhile to investigate whether these isoniazid and pyrazinamide-based complexes also act by the same mechanism. β-Haematin is a synthetic form of haemozoin and is the target of many quinoline-containing compounds like CQ.[56,57] Haemozoin crystal growth inhibition occurs in the digestive vacuole of the parasite. Quinolines can bind to haematin (ferriprotoporphyrin IX), a toxic by-product of haemoglobin degradation which prevents conversion into haemozoin, which is less toxic. The parasite then dies owing to a build-up of ferriprotoporphyrin IX.[56,57] β-Haematin formation can be monitored using the NP-40 detergent-mediated assay. NP-40, a neutral detergent, is used to resemble lipids and brings about β-haematin formation in the assay. Haemozoin formation is not spontaneous and it is believed that haem crystallisation occurs in the presence of neutral lipids inside of the digestive vacuole of the parasite.[58,59]

The results of the β-haematin inhibition assay are shown in Figure 3. Interestingly, isoniazid did not inhibit β-haematin formation at the highest tested concentration (500 µM). This was consistent with the anitiplasmodial activity data as isoniazid did not exhibit any appreciable antiplasmodial activity. Complex **8** exhibited the highest inhibition of β-haematin formation of the tested compounds, followed by complexes **4** and **3**. It was clearly evident that incorporating ferrocene into these systems resulted in an enhancement in β-haematin inhibition. In fact, incorporation of the second PGM metal, further enhanced the ability of the compound to inhibit β-haematin formation. From the data, it can be proposed that the antiplasmodial activity of some of the complexes may be related to their ability to target haemozoin in the digestive vacuole of the parasite.

View Article Online
DOI: 10.1039/C7DT01053A

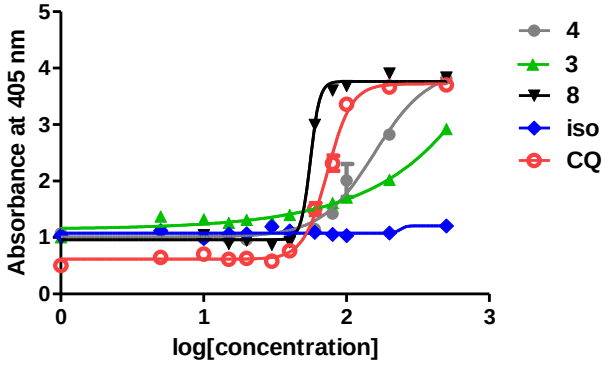

Figure 3 β-Haematin inhibition studies of selected compounds (**3**, **4**, **8**, isoniazid and CQ).

Experimental

Materials. Synthetic procedures were performed under an argon atmosphere at ambient temperatures unless otherwise stated. All reagents were purchased from Sigma Aldrich and used as received. Solvents were dried over Fluka Molecular Sieves with indicator. Pyrazinoic acid hydrazide,[35,36] methyl pyrazinoate,[35,36] the ferrocenyl aldehydes[20,27]and compound **1**[37] were prepared according to literature methods.

Instrumentation and Methods. Nuclear magnetic resonance (NMR) spectra were recorded on a Varian Unity XR400 spectrometer (^{1}H: 399.95 MHz, ^{13}C{^{1}H}: 100.58 MHz), Varian Mercury XR300 spectrometer (^{1}H: 300.08 MHz, ^{13}C{^{1}H}: 75.46 MHz) or Bruker Ultrashield 400 Plus spectrometer (^{1}H: 400.20 MHz, ^{13}C{^{1}H}: 100.60 MHz) at 30.0°C using tetramethylsilane (TMS) as the internal standard. Infrared (IR) absorptions were measured on a PerkinElmer Spectrum One FT-IR spectrometer and samples were analysed using attenuated total reflectance (ATR). EI or ESI-mass spectrometry was used to further characterize all new compounds and determinations were carried out using a JEOL GCmateII mass or a Waters API Quattro instrument in the positive mode, respectively. Purity was checked using an analytical Agilent HPLC 1260 equipped with an Agilent DAD 1260 UV/vis detector and a X Bridge C18 column (2.5 mM, 50 mm X 3 mm) or a Agilent HPLC 1220 using a Kinetex C18 column. The compounds were eluted using a mixture of solvent A (10 mM NH_4OAc/H_2O) and solvent B (10 mM NH_4OAc/MeOH) at a flow rate of 0.9 mL min^{-1}. The gradient elution conditions were as follows: 10% solvent B between 0 and 1 min, 10-95% solvent B between 1 and 3 min, 95% solvent B between 3 and 5 min. In some cases, isocratic conditions were used ACN:H_2O (50%). Elemental analyses were carried out using a Fisions EA 110 elemental analyser.

Synthesis. *General procedure for compounds* ***2****-****6.*** To a stirred solution of the appropriate hydrazide (1 eq.) in EtOH, the appropriate ferrocenyl aldehyde (1 eq.) was added. The resulting solution was refluxed for 24 hours, yielding (after cooling) a red/orange precipitate. The precipitate was then filtered, washed with ethanol, followed by *n*-pentane and dried *in vacuo*.

Compound ***2.*** Isonicotinylhydrazide (47.2 mg, 0.344 mmol) and ferrocenylbenzaldehyde (**B**) (106 mg, 0.357 mmol) were reacted and yielded the product as a red amorphous solid (83.4 mg, 56%). ^{1}H NMR (300.08 MHz, DMSO-d_6): (δ, ppm) 4.17 (5H, s, Cp); 4.36 (2H, br s, Cp); 4.61 (2H, br s, Cp); 6.83 (1H, d, *J* = 16, C=CH); 7.13 (1H, d, *J* = 16, C=CH); 7.59 (2H, d, *J* = 8, ArH); 7.72 (2H, d, *J* = 8, ArH); 7.84 (2H, d, *J* = 5, ArH); 8.46 (1H, s, HC=N); 8.79 (2H, d, *J* = 5, ArH); 12.06 (1H, s, NH). ^{13}C{^{1}H} NMR (100.64 MHz, DMSO-d_6): (δ, ppm) 67.5; 69.5; 69.7; 83.3; 121.9; 125.4; 126.5; 128.2; 129.4; 132.7; 140.2; 141.0; 149.3; 150.8; 162.01. IR (ATR): (υ, cm^{-1}) 1663; 1605; 1592. Microanalysis calculated for $C_{25}H_{21}N_3OFe{\cdot}1H_2O$: C, 64.95; H, 5.23; found C, 65.17; H, 4.81. EI-MS: m/z 435 ([M]$^+$, $C_{25}H_{21}N_3OFe$).

Compound ***3.*** Isonicotinyl hydrazide (43.4 mg, 0.316 mmol) and ferrocenylsalicylaldehyde (**C**) (109 mg, 0.328 mmol) were reacted and yielded the product as a red amorphous solid (48.7 mg, 34%). ^{1}H NMR (300.08 MHz, DMSO-d_6): (δ, ppm) 4.14 (5H, s, Cp); 4.30 (2H, t, *J* = 2, Cp); 4.56 (2H, t, *J* = 2, Cp); 6.75 (1H, d, *J* = 16, C=CH); 6.85 (1H, d, *J* = 16, C=CH); 6.93 (1H, d, *J* = 8, ArH); 7.49 (1H, dd, *J* = 8, *J* = 2, ArH); 7.72 (1H, d, *J* = 2, ArH); 7.86 (2H, d, *J* = 6, ArH); 8.71 (1H, s, HC=N); 8.81 (1H, d, *J* = 6, ArH); 11.09 (1H, s, OH); 12.28 (1H, s, NH). ^{13}C{^{1}H} NMR (100.64 MHz, DMSO-d_6): (δ, ppm) 66.9, 69.1, 69.4, 84.1, 117.4, 119.4, 121.9, 125.3, 125.5, 126.5, 129.4, 129.8, 140.6, 149.0, 150.9, 157.0, 161.9. IR (ATR): (υ, cm^{-1}) 1652, 1619, 1607, 1584. Microanalysis calculated for: $C_{25}H_{21}N_3O_2Fe{\cdot}0.5H_2O$ C, 65.23; H, 4.82; found C, 65.43; H, 4.64. EI-MS: m/z 451 ([M]$^+$, $C_{25}H_{21}N_3O_2Fe$).

Compound ***4.*** Pyrazinyl hydrazide (110 mg, 0.793 mmol) and ferrocenecarboxaldehyde (**A**) (178 mg, 0.832 mmol) were reacted and yielded the product as an orange amorphous solid (137 mg, 52%). ^{1}H NMR (300.08 MHz, $CDCl_3$): (δ, ppm) 4.25 (5H, s, Cp); 4.48 (2H, s, Cp); 4.77 (2H, s, Cp); 8.32 (1H, s, ArH); 8.57 (1H, s, HC=N); 8.83 (1H, s, ArH); 9.53 (1H, s, ArH); 10.48 (1H, s, NH).^{13}C{^{1}H} NMR (100.64 MHz, $CDCl_3$): (δ, ppm) 68.5, 69.4, 70.9, 142.4, 144.2, 144.9, 147.6, 151.9, 158.2. IR (ATR): (υ, cm^{-1}) 1684, 1611, 1580. Microanalysis calculated for $C_{16}H_{14}N_4OFe$: C, 57.51; H, 4.22; found C, 57.16; H, 3.97. EI-MS: m/z 334 ([M]$^+$, $C_{16}H_{14}N_4OFe$).

Compound ***5.*** Pyrazinyl hydrazide (35.3 mg, 0.256 mmol) and ferrocenylbenzaldehyde (**B**) (84.9 mg, 0.268 mmol) were reacted and yielded the product as an orange amorphous solid (57.1 mg, 51%). ^{1}H NMR (300.08 MHz, DMSO-d_6): (δ, ppm) 4.17 (5H, s, Cp); 4.36 (2H, t, *J* = 2, Cp); 4.61 (2H, t, *J* = 2, Cp); 6.82 (1H, d, *J* = 16, C=CH); 7.12 (1H, d, *J* = 16, C=CH); 7.59 (2H, d, *J* = 8, ArH); 7.70 (2H, d, *J* = 8, ArH); 8.63 (1H, s, HC=N); 8.80 (1H, m, ArH); 8.94 (1H, d, *J* = 2, ArH); 9.28 (1H, d, *J* = 1, ArH); 12.25 (1H, s, NH). ^{13}C{^{1}H} NMR (100.64 MHz, DMSO-d_6): (δ, ppm) 67.5; 69.5; 69.7; 83.3; 125.4; 126.5; 128.2; 129.4; 132.8; 140.2; 143.8; 144.6; 145.2; 148.3; 150.1; 159.9. IR (ATR): (υ, cm^{-1}) 1682, 1663, 1633, 1592. Microanalysis calculated for $C_{24}H_{20}N_4OFe{\cdot}0.3H_2O$: C, 65.26; H, 4.70; found C, 65.60; H, 4.60. EI-MS: m/z 436 ([M]$^+$, $C_{24}H_{20}N_4OFe$).

Compound ***6.*** Pyrazinyl hydrazide (16.8 mg, 0.121 mmol) and ferrocenylsalicylaldehyde (**C**) (40.3 mg, 0.121 mmol) were reacted and yielded the product as an orange amorphous solid (17.5 mg, 32%). ^{1}H NMR (300.08 MHz, $CDCl_3$): (δ, ppm) 4.21 (5H, s, Cp); 4.37 (2H, s, Cp); 4.55 (2H, s, Cp); 6.57 (1H, d, *J* = 14.40, C=CH); 6.74 (1H, d, *J* = 14.04, C=CH); 7.04 (1H, d, *J* = 8.52, ArH); 7.28 (1H, s, ArH); 7.45 (1H, d, *J* = 8.43, ArH); 8.62 (2H, br s, ArH, HC=N); 8.87 (1H, s, ArH); 9.53 (1H, s, ArH); 10.65 (1H, br s, NH); 10.93 (1H, s, OH). ^{13}C{^{1}H} NMR (100.64 MHz, $CDCl_3$): (δ, ppm) 66.8, 69.0, 69.4, 83.9, 117.2, 117.8, 124.9, 125.4, 128.6, 129.6, 129.8, 142.5, 143.5, 144.9, 148.1, 152.3, 157.9, 158.4. IR (ATR): (υ, cm^{-1}) 1690, 1614, 1584. Microanalysis calculated for $C_{24}H_{20}N_4O_2Fe{\cdot}0.5H_2O$: C, 62.49; H, 4.59; found C, 62.87; H, 4.55. EI-MS: m/z 452 ([M]$^+$, $C_{24}H_{20}N_4O_2Fe$).

General procedure for compounds ***7****-****9.*** To a stirred solution of the ferrocenyl isoniazid ligand (**1**) (2 eq.) in DCM, excess NaH (60% dispersion in mineral oil) was added and the mixture stirred at room temperature for 1.5 hours. After this time, the appropriate metal dimer (1 eq.) was added. The mixture was stirred for another 1.5 hours at room temperature. Approximately 10 mL of MeOH was slowly added and the mixture stirred for an additional 15 minutes. After this time the mixture was filtered, the filtrate collected and the solvent was removed *in vacuo* to give a red residue. Diethyl ether was then added to extract the product and the solution was then filtered to remove any unreacted starting materials. The filtrate was collected, the solvent removed *in vacuo* and the residue washed with petroleum ether. The sample was then dried under vacuum to yield the desired complexes as bright orange powders.

Compound ***7.*** Ferrocenyl isoniazid ligand (**1**) (20.5 mg, 0.0615 mmol), NaH (12.0 mg, 0.500 mmol) and $[Ir(Cp^*)Cl_2]_2$ (25.0 mg, 0.0314 mmol) were reacted to yield the desired product (35.1 mg, 82%). ^{1}H NMR (300.08 MHz, $CDCl_3$): (δ, ppm) 1.52 (15H, s, Cp*); 4.32 (5H, s, Cp); 4.54 (2H, t, *J* = 1.83, Cp); 4.58-4.60 (1H, m, Cp); 5.90 (1H, br s, Cp); 7.98 – 8.01 (2H, m, ArH); 8.65 – 8.69 (3H, m, ArH, HC=N). ^{13}C{^{1}H} NMR (100.64 MHz, $CDCl_3$): (δ, ppm) 9.00; 70.12; 70.44; 71.36; 72.15; 73.06; 77.88; 85.55; 122.75; 139.17; 149.86; 158.81; 171.64. IR (ATR): (υ, cm^{-1}) 1591. Microanalysis calculated for $C_{27}H_{29}N_3OClFeIr$: C, 46.66; H, 4.21; found C, 46.85; H, 4.38. EI-MS: m/z 695 ([M]$^+$, $C_{27}H_{29}N_3OClFeIr$).

Compound ***8.*** Ferrocenyl isoniazid ligand (**1**) (30.3 mg, 0.0909 mmol), NaH (12.2 mg, 0.508 mmol) and $[Rh(Cp^*)Cl_2]_2$ (28.6 mg, 0.0463 mmol) were reacted to yield the desired product (47.1 mg, 86%). ^{1}H NMR (300.08 MHz, $CDCl_3$): (δ, ppm) 1.53 (15H, s, Cp*); 4.32 (5H, s, Cp); 4.51-4.57 (2H, m, Cp); 4.59 (1H, br s, Cp); 6.04 (1H, br s, Cp); 7.94 – 8.03 (2H, m, ArH); 8.60 – 8.72 (3H, m, ArH, HC=N). ^{13}C{^{1}H} NMR (100.64 MHz, $CDCl_3$): (δ, ppm) 9.0; 69.9; 70.1; 71.3; 71.9; 72.7; 78.2; 93.9 (d, *J* = 73); 122.6; 140.9; 149.7; 159.3; 169.6. IR (ATR): (υ, cm^{-1}) 1591. Microanalysis calculated for $C_{27}H_{29}N_3OClFeRh$: C, 53.54; H, 4.83; found C, 53.62; H, 4.32. EI-MS: m/z 605 ([M]$^+$, $C_{27}H_{29}N_3OClFeRh$).

Compound ***9.*** Ferrocenyl isoniazid ligand (**1**) (29.3 mg, 0.0879 mmol), NaH (12.0 mg, 0.500 mmol) and $[Ru(p\text{-cymene})Cl_2]_2$ (26.9 mg, 0.0440 mmol) were reacted to yield the desired product (43.8 mg, 83%). ^{1}H NMR (300.08 MHz, $CDCl_3$): (δ, ppm) 1.13 (3H, d, *J* = 4, CH_3); 1.16 (3H, d, *J* = 4, CH_3); 2.32 (3H, s, CH_3); 2.61 (1H, sept, *J* = 7, CH); 4.31 (5H, s, Cp); 4.55-4.61 (2H, m, Cp); 4.67-4.69 (1H, m, Cp); 4.85 (1H, d, *J* = 6, *p*-cy); 5.10 (1H, d, *J* = 6, *p*-cy); 5.40-5.45 (2H, m, *p*-cy); 5.77 (1H, br s, Cp); 7.93 (2H, d, *J* = 6, ArH); 8.64 (2H, d, *J* = 5, ArH); 8.75 (1H, s, HC=N). ^{13}C{^{1}H} NMR (100.64 MHz, $CDCl_3$): (δ, ppm) 18.9; 21.9; 22.6; 30.9; 69.9; 70.2; 70.9; 711.9; 72.6; 78.9; 80.9; 81.3; 82.1; 84.4; 101.2; 101.6; 122.6; 139.8; 149.7; 160.4; 170.9. IR (ATR): (υ, cm^{-1}) 1590.

Microanalysis calculated for $C_{27}H_{28}N_3OFeRuCl.0.5Et_2O$: C, 54.43; H, 5.20; found C, 54.21; H, 5.42. HR-ESI-MS: m/z 604.0394 ($[M+H]^+$, $[C_{27}H_{28}N_3OFeRuCl+H]^+$, requires 604.0392).

***In vitro* antimycobacterial activity**.

GAST/Fe MIC determinations. The broth microdilution method[60] allows a range of concentrations to be tested using a single 96-well plate to determine the minimum inhibitory concentration (MIC). A 10 mL culture of *Mycobacterium tuberculosis* (H37RvMa)[61] was grown to an OD600 of 0.6 - 0.7. The culture was then diluted 1:100 in GAST/Fe medium. In a 96-well microtitre plate, 50 µL of GAST/Fe medium was added to all wells in rows 2-12. The compounds were added to row 1 in duplicate, at a final concentration of 640 µM (stocks are made up to a concentration of 10 mM in DMSO, and diluted to 640 µM in GAST/Fe medium). A two-fold serial dilution was prepared by transferring 50 µL of the liquid in row 1 to row 2 and was aspirated to mix. 50 µL of the liquid in row 2 was then transferred to row 3 and aspirated, etc. This procedure was repeated until row 12 was reached, from which 50 µL of the liquid was discarded so as to bring the final volume in all wells to 50 µL. Finally, 50 µL of the 1:100 diluted *M. tuberculosis* culture was added to all wells in rows 2-12. Cells were not added to row 1, as this served as a contamination control. Controls included media only, 5% DMSO, and Rifampicin. The microtitre plate was stored in a secondary container and incubated at 37 °C with a humidifier to prevent evaporation of the liquid. The lowest concentration of drug that inhibits growth of more than 90% of the bacterial population is considered to be the MIC_{90}. MIC_{90} and MIC_{99} values were scored visually at 14-days post inoculation.

GFP assay and activity. The minimum inhibitory concentration (MIC) of compounds was determined in either 7H9 (Difco) medium supplemented with 0.05% Tween-80, 0.2% glycerol and albumin/NaCl/ glucose (ADC) complex, and/or in GAST-Fe (glycerol–alanine–salts) medium pH 6.6, supplemented with 0.05% Tween-80.[62] Compounds were dissolved in DMSO to a final stock concentration of 10 mM. MICs against H37RvMa, Δ*cyd*KO and Δ*cyd*KO/A317T mutants[51] were determined using the standard broth microdilution method described previously.[63] MICs against the *Mtb*::*gfp* strain (H37RvMa::pMSP12GFP)[64] were determined as described previously,[65] with some modifications. Briefly, a two-fold serial dilution of the compound was carried out across a 96-well plate from row 2-11 (20-0.039 µM) in 7H9 or GAST-Fe with a final DMSO concentration of 5% v/v. The minimum growth control (rifampicin at 2xMIC) was added to row 12 and the maximum growth control (5% DMSO in 7H9 or GAST-Fe) was added to row 1. A *Mtb*::*gfp* stock culture was grown to an OD600-0.6, diluted (1:500 for 7H9 or 1:100 for GAST/Fe) and 50 µL added to each well. Plates were incubated at 37 °C and fluorescence (excitation 485 nM; emission 520 nM) was measured using a plate reader (FLUOstar OPTIMA, BMG LABTECH) at day 14. Data were normalised to the minimum and maximum inhibition controls to generate a dose response curve (% inhibition) from which the MIC values were calculated.

***The microplate Alamar Blue Assay*.** This assay was used for MIC determination of clinical Δ*cyd*KO and *qcrBA317T* mutant *M. tuberculosis* isolates. The broth microdilution method was adapted to determine the MICs of selected compounds against clinical strains of *M. tuberculosis* in GAST-Fe medium. The activity of the compounds was measured on day 14 by adding 10 µL Alamar Blue (Celtic Diagnostics) to all wells followed by incubation of the plates at 37 °C for 24 hr. Wells were then viewed for a colour change (blue indicated no growth as opposed to pink which suggested bacterial growth). The MIC values were defined as the lowest drug concentration where a colour change was not observed.[66]

***In vitro* antiplasmodial assay.** The samples were tested in triplicate on one experiment against the chloroquine-sensitive NF54 strain and chloroquine-resistant K1 strain of *P. falciparum*. Continuous in vitro cultures of asexual erythrocyte stages of *P. falciparum* were maintained using a modified method of Trager and Jensen.[67] The antiplasmodial activity in vitro was determined via the parasite lactate dehydrogenase assay using a modified method described by Makler *et al*.[68] The samples were prepared as a 2 mg mL^{-1} stock solution using DMSO and sonicated to enhance solubility. Samples were tested as a suspension if not completely dissolved. Stock solutions were stored at 20 °C. Further dilutions were prepared on the day of the experiment. Chloroquine was used as the reference drug in all experiments. A full dose-response measurement was performed for all compounds to determine the concentration inhibiting 50% of parasite growth (IC_{50} value). The samples were tested at a starting concentration of 10 000 ng mL^{-1}, which was then serially diluted 2-fold in complete medium to give 10 concentrations. The same dilution technique was used for all samples. The highest concentration of solvent to which the parasites were exposed to had no measurable effect on the parasite viability. The IC_{50} values were obtained using a nonlinear dose-response curve fitting analysis via Graph Pad Prism v.5.0 software.

***In vitro* antitrichomonal assay.** Cultures of *T. vaginalis* G3 strain were grown in 5 mL complete TYM Diamond's media in a 37 °C incubator for 24 h. 50 mM stocks of the compounds were made by dissolving in DMSO and were screened against G3 stain of *T. vaginalis*. Cells untreated and inoculated with 5 ml DMSO are used as controls. 5 mL of 50 mM stocks of the compound library were inoculated for a final concentration of 50 mM. Results were calculated based on counts utilizing a haemocytometer after 24 h.

In vitro normal flora screening assay. Non-pathogenic normal flora strains such as *Lactobacillus reuteri* (ATCC 23272, *Lactobacillus acidophilus* (ATCC 43560), and *Lactobacillus rhamnosus* (ATCC 53103) were grown in Lactobacilli MRS at 37 °C under anaerobic conditions. 100 mM stock compounds as well as vehicle control DMSO were diluted to 100 mM in media and incubated with empty BDL-sensi-discs (6 mm) for 20 min at room temperature. Discs containing vehicle control, compounds, or various antibiotic discs [levofloxacin (5 µg), gentamicin (10 µg), and gentamicin (120 µg)] were placed onto the bacterial streaked agar plates and incubated overnight at 37 °C. Vehicle, compound, or antibiotic sensitivity was determined via measurement of zones of inhibition around each disc in mm.

***In vitro* cytotoxicity.** Test samples were screened for *in vitro* cytotoxicity against a mammalian cell-line, Chinese Hamster Ovarian (CHO) using the 3-(4,5-dimethylthiazol-2-yl)-2,5-diphenyltetrazolium bromide (MTT)-assay. The MTT-assay is used as a colorimetric assay for cellular growth and survival, and compares well with other available assays.[69,70] The tetrazolium salt MTT was used to measure all growth and chemosensitivity. The tetrazolium ring is cleaved in active mitochondria. Thus only viable cells are able to reduce the

water-soluble yellow colored MTT to water-insoluble purple colored formazan. Formazan crystals are dissolved in dimethyl sulfoxide (DMSO).The test samples were tested in triplicate on one occasion. The test samples were prepared to a 20 mg mL^{-1} stock solution in 100% DMSO. Stock solutions were stored at 20 °C. Further dilutions were prepared in complete medium on the day of the experiment. Samples were tested as a suspension if not completely dissolved. Emetine was used as the reference drug in all experiments. The initial concentration of emetine was 100 µg mL^{-1}, which was diluted in complete medium with 10-fold dilutions to give 6 concentrations, the lowest being 0.001 µg mL^{-1}. The same dilution technique was applied to all test samples. The highest concentration of solvent to which the cells were exposed to had no measurable effect on the cell viability. The 50% inhibitory concentration (IC_{50}) values were obtained from full dose–response curves, using a non-linear dose–response curve fitting analysis via GraphPad Prism v.5 software.

β-Haematin inhibition assay. The β-haematin assay was adapted from the method described by Wright and co-workers.[55] Compounds were prepared as a 10 mM stock solution in 100% DMSO. Samples were tested at a starting concentration of 500 µM and the lowest drug concentration was 5 µM. The stock solution was serially diluted to give 12 concentrations in a 96 well flat-bottom assay plate. NP-40 detergent was then added to mediate the formation of β-haematin (30.55 µM, final concentration). A 25 mM stock solution of haematin was prepared by dissolving hemin (16.3 mg) in dimethyl sulfoxide (1 mL). A 177.76 µL aliquot of haematin stock was suspended in 20 mL of a 2 M acetate buffer, pH 4.7. The haematin suspension was then added to the plate to give a final haematin concentration of 100 µM. The plate was then incubated for 16 hours at 37 °C. The compounds were analysed using the pyridineferrochrome method developed by Ncokazi and Egan.[71] 32 µL of a solution of 50% pyridine, 20% acetone, 20% water, and 10% 2M HEPES buffer (pH 7.4) was added to each well. To this, 60 µL acetone was then added to each well and mixed. The absorbance of the resulting complex was measured at 405 nm on a SpectraMax 340PC plate reader. The IC_{50} values were obtained using a non-linear dose-response curve fitting analysis via Graph Pad Prism v.5.0 software.

Conclusions

A small family of isonicotinyl and pyrazinamide-derived ferrocenyl complexes was prepared by simple Schiff-base condensation reactions with the aim of investigating the effect on antimicrobial activity when incorporating ferrocene as part of these systems. Three half-sandwich PGM complexes containing iridium, rhodium and ruthenium were also prepared to investigate the effect on biological activity when incorporating these metals. The compounds were tested for antimycobacterial, antiplasmodial and antitrichomonal activity. The compounds were found to possess relatively low cytotoxicity against CHO cells, which suggests selectivity as antimicrobial agents. Most of the compounds exhibited promising antimycobacterial activity. The platinum group metal complexes exhibit a glycerol-dependent activity which might allude to a specific mechanism of action. In the case of antiplasmodial activity, some of the compounds exhibit only moderate activity, lower than the reference drug, chloroquine. However, incorporation of the ferrocenyl moiety (specifically the salicylaldimine moiety) improves the antiplasmodial activity compared to the organic analogue (isoniazid). Complexes with higher lipophilicity also show enhanced antiplasmodial activity. Selected compounds do exhibit the ability to inhibit synthetic haemozoin formation, which may be a contributing mechanism to the antiplasmoidal effects. The same phenomenon is observed for the antitrichomonal activity. Only two compounds exhibited parasite growth inhibition above 80%. From this, it can be concluded that these complexes show promising activity as potential antimycobacterial agents. Further work to elucidate a mechanism of action of these complexes and the role that the ferrocenyl moiety plays is thus required. In addition to this, optimization of the antimycobacterial activity in various media is also required.

Acknowledgements

Financial support from the University of Cape Town, the National Research Foundation (NRF; Grant Number: 90500) and the South African Medical Research Council (MRC) is gratefully acknowledged. Professor Timothy J. Egan (UCT) is gratefully acknowledged for his assistance with the β-haematin inhibition assay. CT and LWC were funded by the U. S. Department of Agriculture, Agricultural Research Service (National Program 108, Project CRIS 5325-42000-049-00D). K.M.L. was supported by the Department of Biological Sciences, the University of the Pacific.

Notes

Supporting Information is available for NMR spectra and LC data (PDF). The authors declare no competing financial interest.

References

1 (a) C. G. Hartinger, P. J. Dyson, *Chem. Soc. Rev.*, 2009, **38**, 391-401. (b) D L. Ma, L. J. Liu, K. H. Leung, Y. T. Chen, H. J. Zhong, D. S. Chan, H. M. Wang, C. H. Leung, *Angew Chem Int Ed Engl.*, 2014, **53**, 9178-9182. (c) H. J. Zhong, L. Lu, K. H. Leung, C. C. L. Wong, C. Peng, S. C. Yan, D. L. Ma, Z. Cai, H. M. Wang, C. H. Leung, *Chem. Sci.*, 2015, **6**, 5400-5408. (d) D L. Ma, H. Z. He, K. H. Leung, D. S. Chan, C. H. Leung, *Angew Chem Int Ed Engl.*, 2013, **52**, 7666-7682.

2 (a) Bioorganometallics: Biomolecules, Labeling, Medicine, ed. G. Jaouen, Wiley-VCH, Weinheim, Germany, 2006. (b) D. R. van Staveren, N. Metzler-Nolte, *Chem. Rev.*, 2004, **104**, 5931−5985

3 (a) C. Biot, D. Dive, *Top. Organomet. Chem.*, 2010, **32**, 155-193. (b) A. Wieczorek, A. Błauż, A. Żal, H. J. Arabshahi, J. Reynisson, C. G. Hartinger, B. Rychlik,* D. Plażuk, *Chem. Eur. J.*, 2016, **22**, 11413-11421.

4 Biot, C.; Dive, D. in Medicinal Organometallic Chemistry, ed. G. Jaouen and N. Metzler-Nolte, Springer, 2010, pp. 155.

5 E.M. Lewandowski, L. Szczupak, S. Wong, J. Skiba, A. Guśpiel, J. Solecka, V. Vrček, K. Kowalski, Y. Chen, *Organometallics*, 2017, **36**, 1673-1676.

6 E.M. Lewandowski, J. Skiba, N.J. Torelli, A. Rajnisz, J. Solecka, K. Kowalski, Y. Chen, *Chem. Commun.*, 2015, **51**, 6186-6189.

7 P. Meunier, I. Ouattara, B. Gautheron, J. Tirouflet, D. Camboli, J. Besancon, *Eur. J. Med. Chem.*, 1991, **26**, 351-362.

8 S. Top, J. Tang, A. Vessieres, D. Carrez, C. Provot, G. Jaouen, *Chem. Commun*., 1996, **8**, 955-956.
9 P. Köpf-Maier, H. Köpf, E. W. Neuse, *Angew. Chem. Int. Ed. Engl*., 1984, **23**, 456-457.
10 P. Köpf-Maier, H. Köpf, H. *Drugs Future,* 1986, **11**, 297-319.
11 G. Jaouen, A. Vessieres, S. Top, *Chem. Soc. Rev*., 2015, **44**, 8802-8817.
12 E. Hillard, A. Vessieres, L. Thouin, G. Jaouen, C. Amatore, *Angew. Chem. Int. Ed*., 2006, **45**, 285-290.
13 Y. Wang, M. –A. Richard, S. Top, P. M. Dansette, P. Pigeon, A. Vessieres, D. Mansuy, G. Jaouen, *Angew. Chem. Int. Ed.*, 2016, **55**, 10431-10434.
14 T. Wang, P. Pigeon, M. J. McGlinchey, S. Top, G. Jaouen, *J. Organomet. Chem*., 2017, **829**, 108-115.
15 J. Hess, M. Patra, L. Rangasamy, S. Konatschnig, O. Blacque, A. Jabbar, P. Mac, E. M. Jorgensen, R. B. Gasser, G. Gasser, *Chem. Eur. J.* 2016, **22**, 16602-16612
16 J. Hess, M. Patra, V. Pierroz, B. Spingler, A. Jabbar, S. Ferrari, R. B. Gasser, G. Gasser, *Organometallics*, 2016, **35**, 3369−3377.
17 World Health Organization, Global Tuberculosis Report 2016; <http://www.who.int/tb/publications/global_report/en/>
18 A. Koul, E. Arnoult, N. Lounis, J. Guillemont, K. Andries, *Nature*, 2011, **469**, 483-490.
19 D. Razafimahefa, D. A. Ralambomanana, L. Hammouche, L. Pe´linski, S. Lauvagie, C. Bebear, J. Brocard, J. Maugeind, *Bioorg. Med. Chem. Lett*., 2005, **15**, 2301-2303.
20 N. Baartzes, T. Stringer, R. Seldon, D. F. Warner, C. de Kock, P. J. Smith, G. S. Smith, *J. Organomet. Chem.,* 2016, **809**, 79-85.
21 S. L. Cudmore, K.L. Delgaty, S. F. Hayword-McClelland, D. P. Petrin, G.E. Garber, *Clin. Microbiol. Rev*., 2004, **17**, 783-793.
22 J. R. Schwebke, D. Burgess, *Clin. Microbiol. Rev*., 2004, **17**, 794-803.
23 J. Kühnert, P. Ecorchard, H. Lang, *Eur. J. Inorg. Chem*., 2008, **32**, 5125-5137.
24 S. Kocher, B. Walfort, G. P. M. van Klink, G. van Koten, H. Lang, *J. Organomet. Chem*., 2006, **691**, 3955-3961.
25 T. Stringer, D. Taylor, C. de Kock, H. Guzgay, A. Au, S. H. An, B. Sanchez, R. O'Connor, N. Patel, K. M. Land, P. J. Smith, D. T. Hendricks, T. J. Egan, G. S. Smith, *Eur. J. Med. Chem*., 2013, **69**, 90-98.
26 T. Stringer, H. Guzgay, J. M. Combrinck, M. Hopper, D. T. Hendricks, P. J. Smith, K. M. Land, T. J. Egan, G. S. Smith, *J. Organomet. Chem.,* 2015, **788**, 1-8.
27 T. Stringer, C. De Kock, H. Guzgay, J. Okombo, J. Liu , S. Kanetake, J. Kim, C. Tam, L. W. Cheng, P. J. Smith, D. T. Hendricks, K. M. Land, T. J. Egan, G. S. Smith, *Dalton Trans*., 2016, **45**, 13415-13426.
28 M. Adams, C. de Kock, P. J. Smith, K.M. Land, N. Liu, M. Hopper, A. Hsiao, A. R. Burgoyne, T. Stringer, M. Meyer, L. Wiesner, K. Chibale, G. S. Smith, *Dalton Trans*., 2015, **44**, 2456-2468.
29 The World Health Organisation, World Malaria Report 2014 http://www.who.int/malaria/media/world_malaria_report_2014/en/.
30 C. Biot, G. Glorian, L. A. Macejewski, J. S. Brocard, O. Domarle, G. Blampain, P. Millet, A. J. Georges, H. Abessolo, D. Dive, *J. Med. Chem*., 1997, **40**, 3715-3718.
31 G. Mombo-Ngoma, C. Supan, M. P. Dal-Bianco, M.A. Missinou, P. B. Matsiegui, C. L. O. Salazar, S. Issifou, D. Ter-Minassian, M. Ramharter, M. Kombila, P. G. Kremsner, B. Lell, *Malar. J.*, 2011, **10**, 53.
32 C. Biot, W. Castro, C. Y. Botte, M. Navarro, *Dalton Trans*., 2012, **41**, 6335-6345.
33 M. Navarro, M. Castro, C. Biot, *Organometallics,* 2012, **31**, 5715-5725.
34 P. F. Salas, C. Herrmann, C. Orvig, *Chem. Rev.*, 2013, **113**, 3450-3492.
35 F. Zhang, F.; Wen, Q.; Wang, S. –F.; Karim, B. S.; Yang, Y. –S.; Liu, J.-J.; Zhang, W.-M.; Zhu, H.-L. Bioorg. Med. Chem. Lett. 2014, 24, 90-95.
36 M. S. R. Murty, R. Penthala, S. Polepalli, N. Jain, *Med. Chem. Res*., 2016, **25**, 627-643.
37 G. M. Maguene, J. Jakhlal, M. Ladyman, A. Vallin, D. A. Ralambomanana, T. Bousquet, J. Maugein, J. Lebibi, L. Pélinski, *European J. Med. Chem*., 2011, **46**, 31-38.
38 M. R. Valderrama, R. V. García, T. Klimova, E. Klimova, L. Ortiz-Frade, M. M. García, *Inorg. Chim. Acta*, 2008, **361**, 1597-1605.
39 P. Govender, N. C. Antonels, J. Mattsson, A. K. Renfrew, P. J. Dyson, J. R. Moss, B. Therrien, G. S. Smith, *J. Organomet. Chem.*, 2009, **694**, 3470-3476.
40 P. Govender, A. K. Renfrew, C. M. Clavel, P.J. Dyson, B. Therrien, G. S. Smith, *Dalton Trans*., 2011, **40**, 1158-1167.
41 P. Govender, L. C. Sudding, C. M. Clavel, P. J. Dyson, B. Therrien, G. S. Smith, *Dalton Trans*., 2013, **42**, 1267-1277.
42 E. Ekengard, L. Glans, I. Cassells, T. Fogeron, P. Govender, T. Stringer, P. Chellan, G. C. Lisensky, W. H. Hersh, I. Doverbratt, S. Lidin, C. de Kock, P. J. Smith, G. S. Smith, E. Nordlander, *Dalton Trans*., 2015, **44**, 19314-19329.
43 W. Nkoana, D. Nyoni, P. Chellan, T. Stringer, D. Taylor, P. J. Smith, A. T. Hutton, G. S. Smith, *J. Organomet. Chem*., 2014, **752**, 67-75.
44 M. Adams, Y. Li, H. Khot, C. de Kock, P. J. Smith, K. M. Land, K. Chibale, G. S. Smith, *Dalton Trans*., 2013, **42**, 4677-4685.
45 T. Stringer, B. Therrien, D. T. Hendricks, H. Guzgay, G. S. Smith, *Inorg. Chem. Commun*., 2011, **14**, 956-960.
46 H. Nikaido, *Biochim. Biophys. Acta*, 1961, **48**, 460-469.
47 T. Fukasawa, H. Nikaido, *Biochim. Biophys. Acta*, 1961, **48**, 470-483.
48 K. Kurahashi, A. J. Wahba, *Biochim. Biophys. Acta*, 1958, **30**, 298-302.
49 N. R. Cozzarelli, J. P. Koch, S. Hayashi , E. C. Lin, *J. Bacteriol*., 1965, **90**, 1325-1329.
50 K. Pethe, P. C. Sequeira, S. Agarwalla, K. Rhee, K. Kuhen, W. Y. Phong, V. Patel, D. Beer, J. R. Walker, J. Duraiswamy, J. Jiricek, T. H. Keller, A. Chatterjee, M. P. Tan, M. Ujjini, S. P. Rao, L. Camacho, P. Bifani, P. A. Mak, I. Ma, S. W. Barnes, Z. Chen, D. Plouffe, P. Thayalan, S. Hwee Ng, M. Au, B. H. Lee, B. H.; Tan, S. Ravindran, M. Nanjundappa, X. Lin, A. Goh, S. B. Lakshminarayana, C. Shoen, M. Cynamon, B. Kreiswirth, V. Dartois, E. C. Peters, R. Glynne, S. Brenner, T. Dick, *Nat. Commun*., 2010, **1**, 1-8.
51 K. Arora, B. Ochoa-Montano, P. S. Tsang, T. L. Blundell, S. S. Dawes, V. Mizrahi, T. Bayliss, C. J. MacKenzie, L. A. T. Cleghorn, P. C. Ray, P. G. Wyatt, E. Uh, J. Lee, C. E. Barry, H. I. Boshoff, *Antimicrob. Agents Chemother*., 2014, **58**, 6962−6965.

View Article Online
DOI: 10.1039/C7DT01058A

View Article Online
DOI: 10.1039/C7DT01952A

52 R. van der Westhuyzen, S. Winks, C. R. Wilson, G. A. Boyle, R. K. Gessner, C. Soares de Melo, D. Taylor, C. de Kock, M. Njoroge, C. Brunschwig, N. Lawrence, S. P. S. Rao, F. Sirgel, P. van Helden, R. Seldon, A. Moosa, D.F. Warner, L. Arista, U. H. Manjunatha, P. W. Smith, L. J. Street, K. Chibale, *J. Med. Chem.*, 2015, **58**, 9371-9381.
53 P. Durel, V. Roiron, A. Siboulet, L. J. Borel, *Br. J. Vener. Dis*., 1960, **36**, 21-26.
54 Centers for Disease Control and Prevention. 1993. Sexually transmitted diseases treatment guidelines. https://www.cdc.gov/mmwr/preview/mmwrhtml/00023296.htm
55 R. D. Sandlin, M. D. Carter, P. J. Lee, J. M. Auschwitz, S. E. Leed, J. D. Johnson, D. W. Wright, *Antimicrob. agents chemother*., 2011, **55**, 3363-3369.
56 N. Sunduru, K. Srivastava, S. Rajakumar, S. K. Puri, J. K. Saxena, P. M. S. Chauhan, *Bioorg. Med. Chem. Lett.,* 2009, **19**, 2570-2573.
57 R. Buller, M. L. Peterson, O. Almarrson, L. Leiserowitz, *Cryst. Growth Des.,* 2002, **2**, 553-562.
58 A. N. Hoang, K. K. Ncokazi, K. A. de Villiers, D. W. Wright, T. J. Egan, *Dalton Trans*., 2010, **39**, 1235-1244.
59 A. N. Hoang, R. D. Sandlin, A. Omar, T. J. Egan, D. W. Wright, Biochemistry, 2010, **49**, 10107-10116.
60 (a) L. Collins, S. G. Franzblau, *Antimicrob. Agents Chemother*., 1997, **41**, 1004-1009; (b) L. A. Collins, M. N. Torrero, S. G. Franzblau, *Antimicrob. Agents Chemother*., 1998, **42**, 344-347.
61 T. R. Ioerger, Y. Feng, K. Ganesula, X. Chen, K. M. Dobos, S. Fortune, W. R. Jacobs Jr., V. Mizrahi, T. Parish, E. Rubin, C. Sassetti, J. C. Sacchettini, *J. Bacteriol*., 2010, **192**, 3645-3653.
62 J.J. De Vos, K. Rutter, B. G. Schroeder, H. Su, Y. Zhu, C. E. Barry, 3rd, *Proc. Natl. Acad. Sci. U S A*, 2000, **97**, 1252-1257.
63 M. Tukulula, R. –K. Sharma, M. Meurillon, A. Mahajan, K. Naran, D. Warner, J. Huang, B. Mekonnen, K. Chibale, *Med. Chem. Lett.,* 2013, **4**, 128-131.
64 G. L. Abrahams, A. Kumar, S. Savvi, A. W. Hung, S. Wen, C. Abell, C. E. Barry, 3rd, D. R. Sherman, H. I. Boshoff, V. Mizrahi, *Chem. Biol*., 2012, **19**, 844-854.
65 J. Ollinger, M. A. Bailey, G. C. Moraski, A. Casey, S. Florio, T. Alling, M. J. Miller, T. Parish, *PloS one*, 2013, **8**, e60531.
66 S. G. Franzblau, R. S. Witzig, J. C. McLaughlin, P. Torres, G. Madico, A. Hernandez, M. T. Degnan, M. B. Cook, V. K. Quenzer, R. M. Ferguson, R. H. Gilman, *J. Clin. Microbiol*., 1998, **36**, 362-366.
67 W. Trager, J. B. Jensen, *Science*, 1976, **193**, 673-675.
68 M. T. Makler, J. M. Ries, J. A. Williams, J. E. Bancroft, R. C. Piper, B. L. Gibbins, D. J. Hinrichs, *Am. J. Trop. Med. Hyg.,* 1993, **48**, 739-741.
69 T. J. Mosmann, *Immunol. Methods*, 1983, **65**, 55-63.
70 L. V. Rubinstein, R. H. Shoemaker, K. D. Paull, R. M. Simon, S. Tosini, P. Skehan, D. A. Scudiero, A. Monks, M. R. Boyd, *J. Natl. Cancer Inst*., 1990, **82**, 1113-1118.
71 K. K. Ncokazi, T. J. Egan, *Anal. Biochem*., 2005, **338**, 306-319.

View Article Online
DOI: 10.1039/C7DT01952A

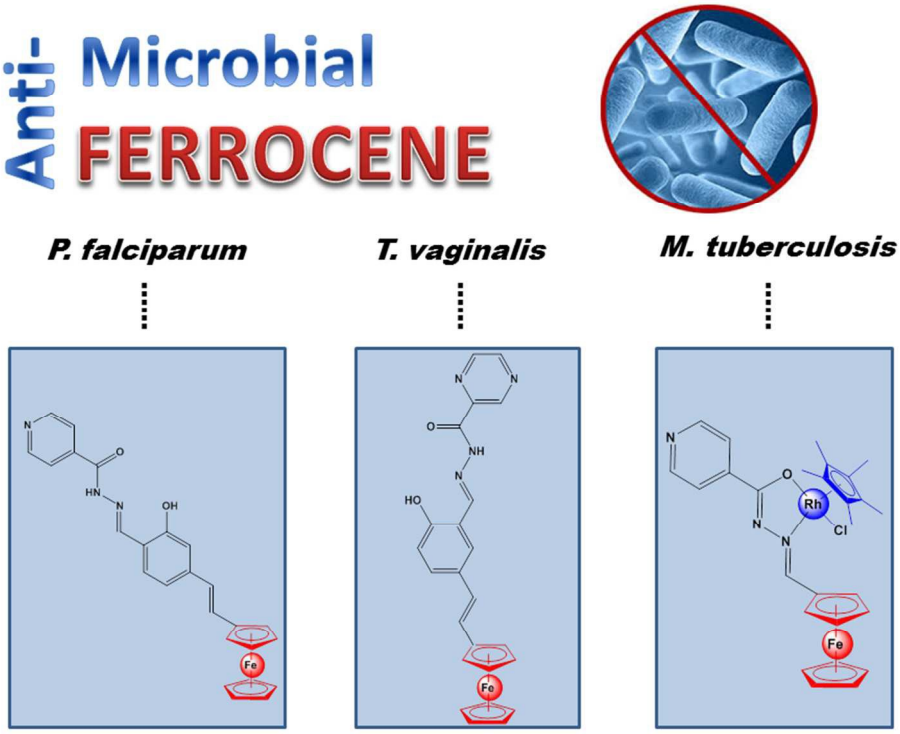

254x190mm (96 x 96 DPI)